

See discussions, stats, and author profiles for this publication at: <https://www.researchgate.net/publication/260255501>

Conductivity and Wettability Changes of Ultrathin Nafion Films Subjected to Thermal Annealing and Liquid Water Exposure

ARTICLE *in* THE JOURNAL OF PHYSICAL CHEMISTRY C · JANUARY 2014

Impact Factor: 4.77 · DOI: 10.1021/jp410510x

CITATIONS

11

READS

94

2 AUTHORS, INCLUDING:



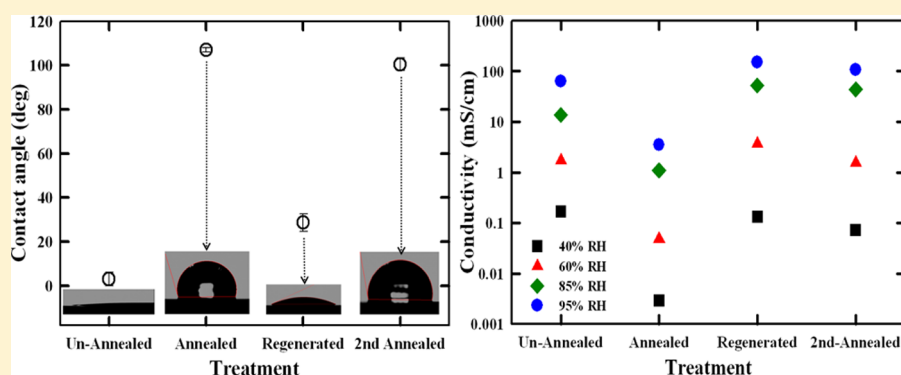
Devproshad K. Paul

The University of Calgary

23 PUBLICATIONS 372 CITATIONS

SEE PROFILE

Conductivity and Wettability Changes of Ultrathin Nafion Films Subjected to Thermal Annealing and Liquid Water Exposure

Devproshad K. Paul^{†,‡,§} and Kunal Karan^{*,†,‡,§}[†]Department of Chemical Engineering, Queen's University, 19 Division Street, Kingston, Ontario K7L 3N6, Canada[‡]Queen's-RMC Fuel Cell Research Centre, Queen's University, 945 Princess Street, Kingston, Ontario K7L 3N6, Canada[§]Department of Chemical and Petroleum Engineering, The University of Calgary, 2500 University Drive N.W., Calgary, Alberta T2N1N4, Canada

ABSTRACT: The ionomer in the catalyst layer of polymer electrolyte fuel cells exists as ultrathin films (4–10 nm) covering the aggregates of Pt/C catalyst and may experience elevated temperatures during hot-pressing step of the electrode fabrication process. In this study, we report the effect of thermal annealing on pertinent ionomer-film properties: proton transport and surface wettability. Self-assembled, 10 nm thin Nafion ionomer films on silica substrate were heat treated at different temperatures in the range 40–160 °C. It was found that both surface and bulk rearrangement/reorganization occur simultaneously upon annealing. Surface reorganization was evident by the dramatic change in free-surface wettability from super-hydrophilic to hydrophobic. On the other hand, bulk rearrangement was evident from significant depression in the proton conductivity with increasing treatment temperature. Extended exposure, up to 18 h, to water in vapor form at high humidity did not change the protonic conductivity. On the other hand, exposure to liquid water resulted in an interesting finding of simultaneous regeneration of the film surface and bulk properties. The latter has implications for *in operando* behavior of ionomer in PEFC cathode catalyst layers, where local water and heat generation may strongly influence its properties.

INTRODUCTION

In recent years, there has been considerable interest in understanding the structure and properties of the ionomer in the catalyst layer (CL) of a polymer electrolyte fuel cell (PEFC).¹ The most widely employed ionomer is perfluorosulfonic acid, available under the name Nafion, a DuPont product. Although the ionomer in the CL and the electrolyte membrane may have similar chemical form, they differ in the characteristic thickness. In the conventional CLs based on Pt/C catalysts, the ionomer forms a thin coating of thickness 4–10 nm over the catalyst aggregate.² In contrast, the polymer electrolytes have thickness in excess of 25 μm , more than 3 orders of magnitude greater than the thin films. Recent studies,^{3–14} including those from our group,^{8,14} indicate that the structure and properties of the supported, Nafion thin films may differ significantly from those of the well-studied, free-standing membrane form of Nafion. The ionic domains in the membranes¹⁵ are of the size (~ 4 –5 nm) comparable to the thickness of the thin film itself, raising questions regarding the

differences in proton conductivity of Nafion thin films and membranes. Further, for ultrathin films the ionomer interaction with the substrate may play an important role in defining its structure and, thereby, its properties.^{4,7,12,16} The difficulty in directly probing the ionomer structure/property in the 5–20 μm thin CL with a porous composite structure has led to studies of thin ionomer films on well-defined planar substrates.^{3,14,16} A clearer picture of the ionomer structure and property may emerge in the coming years as the effects of influencing factors including fabrication method,^{10,11,14} solution/dispersion characteristics,^{14,17,18} substrate type,^{4,16} and thermal annealing^{10,12} are systematically studied. The scope of this paper is restricted to the thermal annealing effects to the most commonly employed perfluorosulfonate ionomer in PEFCs, Nafion.

Received: October 24, 2013

Revised: December 31, 2013

Published: January 3, 2014



The CL undergoes a hot-pressing step, i.e., simultaneous pressing and heating up, during the membrane electrode assembly (MEA) fabrication process to improve the contact between the various components of the MEA, i.e., the porous transport layer or gas diffusion layer, the catalyst layer, and the membrane. During the hot pressing stage, the MEA is placed between hot plates set at temperatures exceeding the glass transition temperature (T_g) of the bulk polymer electrolyte (Nafion bulk $T_g = 109\text{ }^\circ\text{C}$).^{20–22} The influence of this thermal treatment on the structure/property of ionomer in the CL is not known. In general, morphology changes occur when polymers are thermally annealed above its T_g . For very thin polymer films, its interaction with substrate can result in film T_g differing significantly from that of the bulk.^{23,24} Confined by substrate on one side but free to move on the other side, thin polymer films can be expected to exhibit annealing behavior different than their bulk counterpart. Thermal annealing of thin films of block copolymers above their glass transition temperature results in increased mobility and rearrangement of chains causing morphology change manifested as increase in crystallinity¹² and dewetting behavior.^{25,26} Only a few studies on thermal annealing of Nafion thin films are available in the literature.^{10,12,27} It was found that a crystalline domain was formed in 100 nm Nafion film upon annealing at 200 $^\circ\text{C}$. It was proposed that the crystallinity, characterized by scattering peak of SAXS at $q = 0.55\text{ nm}^{-1}$, may restrict water uptake and as such water-mediated proton transport properties.¹² In another study, the dewetting behavior of Nafion ionomer thin films on SiO_2 with thickness ranging from 200 to 400 nm was examined, and no dewetting of the substrate was noted even after prolonged annealing at temperatures above 200 $^\circ\text{C}$,²⁷ contrary to that observed for diblock copolymers.^{28,29}

Recently, we reported that the films of nominal thickness below 55 nm show different surface and bulk characteristics than thicker films.¹⁴ These films were prepared by self-assembly and were not subjected to any thermal treatment step. The effect of annealing on the film properties could be significant. For example, Kongkanand¹⁰ had shown that the kinetics of water uptake of 33–500 nm thick Nafion films was significantly retarded upon thermal annealing and attributed it to the formation of a hydrophobic skin. In this study, we report the effect of thermal annealing on 10 nm thin Nafion films, representative of ionomer film in PEFC catalyst layer. The films were annealed at various temperatures ranging from 40 to 160 $^\circ\text{C}$. Film surface wettability and proton conduction were characterized by water contact angle and impedance spectroscopy measurements, respectively. An interesting part of the study was to examine the effect of exposure of the thermally annealed films to liquid water for extended periods of time to mimic the local environment in a liquid-water flooded CL.

■ EXPERIMENTAL SECTION

Materials and Methods. Thermally grown SiO_2 (thickness $\sim 300\text{ nm}$) on Si wafer was used as the substrate of ultrathin Nafion film preparation. Nafion films were generated by self-assembly using a stock solution of Nafion (EW 1100, 5 wt %) in a water–alcohol mixture (75/20 w/w alcohol to water) obtained from Ion Power. This stock solution was diluted to desired concentrations of 0.25 wt % by addition of isopropyl alcohol (IPA) (Sigma Aldrich). The sample preparation method has been previously described.^{8,14} Briefly, the diluted solutions were sonicated for 5 min and equilibrated for at least 24 h. The silica substrates were immersed into the diluted

Nafion solutions for 12 h to prepare self-assembled Nafion thin films and subsequently dried by N_2 flowing immediately after. The characteristic film thicknesses were measured by three different techniques, namely ellipsometry, atomic force microscope (AFM), and XPS.^{9,14} For EIS measurement, thermally grown SiO_2 (thickness $\sim 2000\text{ nm}$) on Si wafer supporting a comb-shaped interdigitated array (IDA, 110 gold teeth of 0.8 cm length and 100 μm apart) of gold electrodes was used as the substrate. The aforementioned film preparation protocol was adopted for fabricating the Nafion films on IDA.

Ultrathin Film Treatment. The thin films were classified into two categories on the basis of further heat treatment and termed as “unannealed” and “annealed” films. Unannealed films involved two drying steps, (i) 30 min drying under flow of N_2 , immediately after film was removed from the Nafion dispersion after a 12 h immersion, and (ii) drying in a vacuum ($\sim 760\text{ mm}$ of Hg) oven at 40 $^\circ\text{C}$ for 17–20 h. Annealed films were generated by heat treatment of unannealed films at a specified temperature (60–160 $^\circ\text{C}$ range) under vacuum for 1 h. Before the sample was placed in the oven for annealing, the oven was equilibrated at 146 $^\circ\text{C}$ for a 3–4 h period, and temperature was controlled within $\pm 0.5\text{ }^\circ\text{C}$ during the annealing.

For liquid water exposure experiments, a drop of water was placed on the annealed film in such a way that full coverage/contact of the droplet with the film was ensured. The system was equilibrated for 24 h in a humidity chamber set at 100% RH. The high humidity condition minimized the evaporation of liquid water during the prolonged equilibration period. The droplet of water could be still observed at the end of the 24 h equilibration. At the end of the equilibration period, the liquid water was allowed to evaporate at ambient conditions (room temperature and humidity). The water-equilibrated film was dried again by flow of N_2 gas and subjected to the same treatment step as that for “unannealed” film by drying in the vacuum oven for overnight at 40 $^\circ\text{C}$. This film was termed as “regenerated” for reasons that will become apparent in the Results and Discussion section. Again those films were annealed following the same annealing protocol which termed as “2nd annealed” films. All four categorized films were exposed to room temperature after the thermal treatment step and equilibrated with outside atmosphere around 15–30 min before any characterization.

Water Contact Angle Measurement. Water contact angle was measured for all four categorized films by goniometer. The contact angle analyzer was equipped with a video camera and software for image grabbing and analysis. A sessile drop of water of about 0.75 μL large was placed on the top of the surface of both type of unannealed and annealed thin film using a microsyringe. The image was captured within 5 s of the water drop placement on the surface. Several images were also taken every 30 s interval for 5 or more minutes to check the stability of the droplet. It was observed that the contact angle of sessile drop decreases gradually with time; this might happen due to adsorption of water by the polymer or water evaporation. The reported values are the ones obtained within the first $\sim 5\text{ s}$ after placing the drop. The contact angle measurements were conducted at ambient conditions (usually, 25 $^\circ\text{C}$ and 30–50% RH).

Impedance Measurement. Impedance of the four categorized samples was measured following the protocol described in our early publications.^{8,9} Briefly, the IDA with Nafion films was placed in an environmental chamber (model 3911, Thermo Forma) with relative humidity (RH) and

temperature control. The measurements were accomplished by a two microprobe setup connected with a Solartron 1260 frequency-response analyzer coupled to a Solartron 1296 dielectric interface. The measurements were mainly carried out at 60 °C, comparable to fuel cell operating conditions. Moreover, temperature-dependent impedance measurements were also carried out to extract activation energy. During measurement, a humidity sensor (CMOSENS Tec., Switzerland) was placed in the close vicinity of the IDA sample to monitor the local equilibration for RH and temperature. Single-frequency impedance measurements were carried out to monitor the approach to ionomer equilibration. When the impedance value no longer varied, the film was deemed to be equilibrated at the set RH and temperature. At equilibrium condition, impedance data were collected by applying an alternating potential of amplitude 100 mV over a frequency ranging from 10 MHz to 0.01 Hz. Smart impedance measurement software (Solartron Analytical) was used for data collection, and Z-view impedance software (Version 3.0a, Scribner Associates Inc.) was adopted for equivalent-circuit design, model fitting, and data analysis. The film conductivity (κ_f) was calculated from the fitted resistance (R_f) obtained from impedance measurements using eq 1, where d is the space between the IDA electrodes (100 μm), t is the thickness of the film, l is the length of the teeth (0.8 cm), and N is the number of electrodes (110).

$$\kappa_f = \frac{1}{R_f} \cdot \frac{d}{l(N-1)t} \quad (1)$$

■ RESULT AND DISCUSSION

The characterization of the thickness of self-assembled films has been reported elsewhere.^{9,14} Films of reproducible thickness were generated and confirmed by three independent techniques probing different area scales: atomic force microscopy by scratch method examined 1 μm length, variable angle spectroscopic ellipsometry probed 50 μm spot, and X-ray photoelectron spectroscopy probed $2 \times 2 \text{ mm}^2$ sample size.

Proton Conductivity of Annealed and Unannealed Films. The proton conductivities of the unannealed and annealed (at 146 °C) 10 nm Nafion films were determined at 60 °C over a wide range of relative humidity (RH) conditions (20–95% RH). In literature, a wide range of temperature 120–195 °C has reportedly been used as the hot pressing temperature of MEA.²² Hence, a midrange temperature 146–160 °C as a representative temperature of hot pressing was considered to investigate the annealing effect. Later, the annealing temperature effects have also been explored. However, the sample-to-sample variability in the measurements, determined from an average of 3 samples for each film, was within 5% and 10% for unannealed and annealed films, respectively. The proton conductivities as a function of RH are presented in Figure 1. The only other data we could find in the literature is from Siroma's group⁵ who reported the conductivity of the film of the lowest thickness of 14 nm. The extrapolated conductivity data for 10 nm film is also included in Figure 1.

For both unannealed and annealed films, the proton conductivity expectedly increased with an increase in RH. The proton conductivity of unannealed film is consistent with the conductivity reported by Siroma et al.⁵ The apparent difference in conductivity might be due to the differences in the

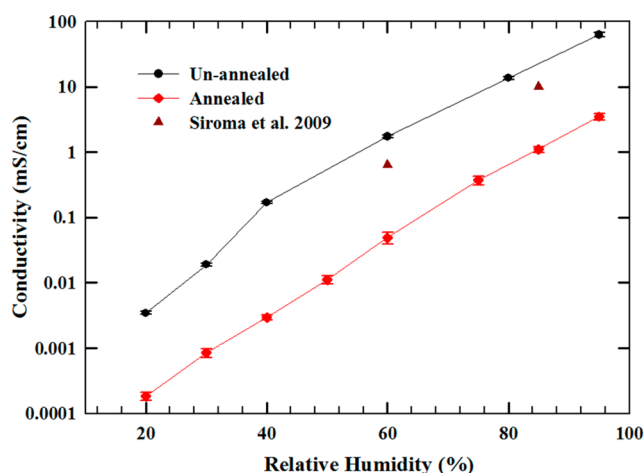


Figure 1. Proton conductivity of both unannealed (black ●) and annealed (red ◆) films at 60 °C and different relative humidity. Proton conductivity data at 85 °C from Siroma et al.⁵ (purple ▲). Error bar represents standard deviation from measurements on triplicate samples.

preparation method and measurement condition. Siroma et al.⁵ employed drop casting for film preparation whereas we have employed self-assembly. Their measurements were performed at 85 °C whereas ours was at 60 °C. Finally, we have used ac impedance spectroscopy whereas Siroma et al. have used a dc based four electrode method. The most notable and a surprising observation is that the proton conductivity of the annealed films is depressed by 1.5–2 orders of magnitude compared to the unannealed film. As stated earlier, data was collected for multiple samples, and results were reproducible. However, to interpret this unexpected result, it was hypothesized that perhaps the 2 h equilibration time was not a sufficiently long time.

Single frequency impedance measurements were performed over an extended period of up to 18 h to investigate whether the film exhibits any significant change in the impedance response. Film impedance was monitored at a fixed frequency of 100 Hz during prolonged exposure of 18 h at relative humidity 95% and 30 °C. After each 6 h equilibration at such a high RH, spectroscopic impedance data was collected over the extended range of frequency (10 MHz to 1 Hz). The film impedance over 18 h is presented in Figure 2 as three different plots representing data over 0–6, 6–12, and 12–18 h. After the first 2 h, the impedance was found to exhibit stable behavior with little fluctuation over the time. Thus, the prolonged exposure of the thermally annealed film to high RH does not change the film resistance and the corresponding proton conductivity after the initial equilibration in the first 2 h.

The conductivity of our unannealed thin film is already lower than the conductivity of bulk Nafion membrane or CL ionomer.⁸ A further reduction in the conductivity of the thin ionomer films upon thermal annealing creates an even larger discrepancy between annealed thin film conductivity and reported CL ionomer conductivity.^{30,31} It was conjectured whether the heat treatment temperature used in our study was significantly higher than that experienced by ionomer during the hot-pressing stage of the MEA preparation that had resulted in damage of the ionomer structure in some manner. It was also of interest to examine the effect of heat treatment at bulk Nafion T_g and far above the T_g . Accordingly, additional conductivity measurements were performed for films heat

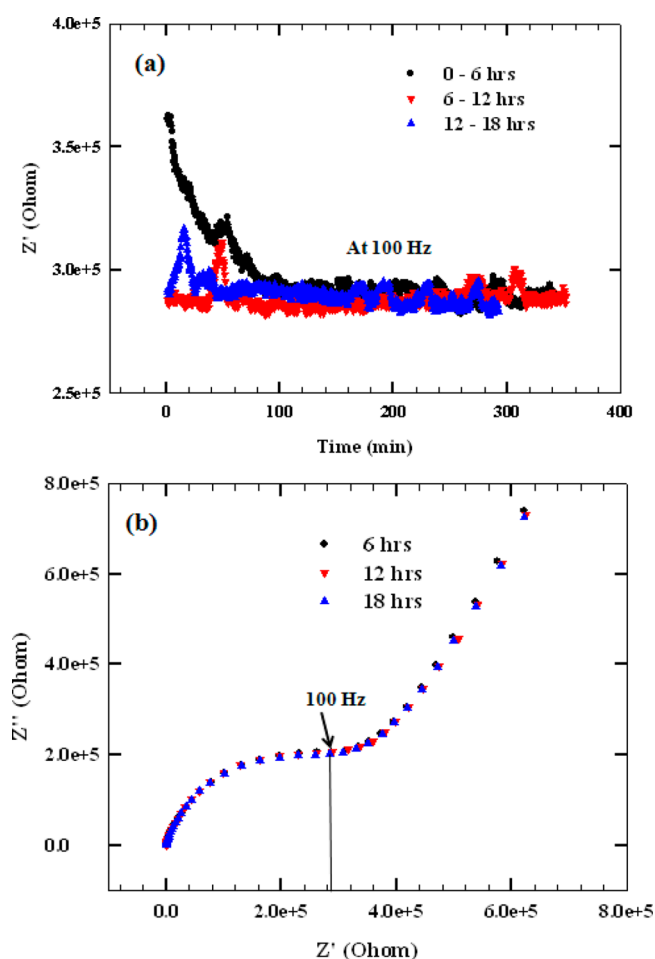


Figure 2. Impedance response of 10 nm Nafion film exposed to 95% RH at 30 °C over 18 h. (a) Fixed frequency (100 Hz) impedance monitored over 360 min (6 h) periods of 0–6 h, 6–12 h, 12–18 h. (b) Impedance spectroscopy data (10 MHz to 1 Hz) after 6, 12, and 18 h exposure.

treated at 110 and 160 °C. As shown in Figure 3 below, even the 110 °C heat-treated film exhibited significantly depressed proton conductivity. On the other hand, the proton

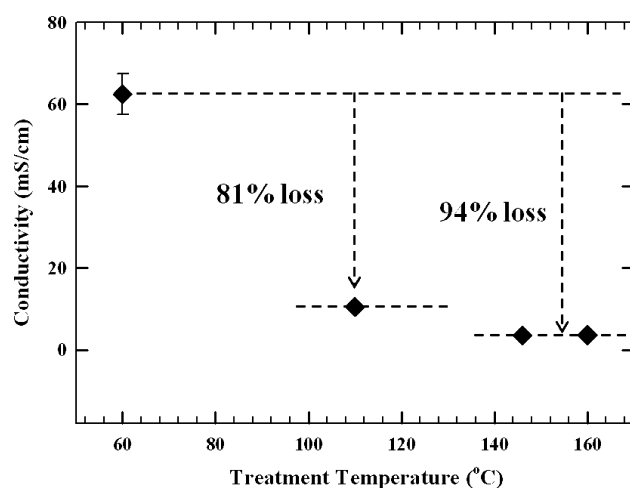


Figure 3. Proton conductivity of annealed ultrathin Nafion film with different film treatment temperature at 95% RH and 60 °C.

conductivity of 160 °C annealed film was essentially the same as that of the 146 °C annealed film.

Effect of Heat Treatment Temperature on Surface Wettability. Significant rearrangement in internal and surface structure can occur for both free-standing and supported films upon thermal treatment. Surface restructuring, which can be probed by changes in wettability, can hold a clue for any internal structure and, thereby, bulk properties (such as conductivity) of the films. The untreated films (vacuum-dried at 40 °C) were heat treated at various temperatures over the range 60–160 °C and the wettability ascertained by water contact angle. The water contact angle for 10 nm Nafion films supported by SiO₂ and heat treated at various temperatures is presented in Figure 4.

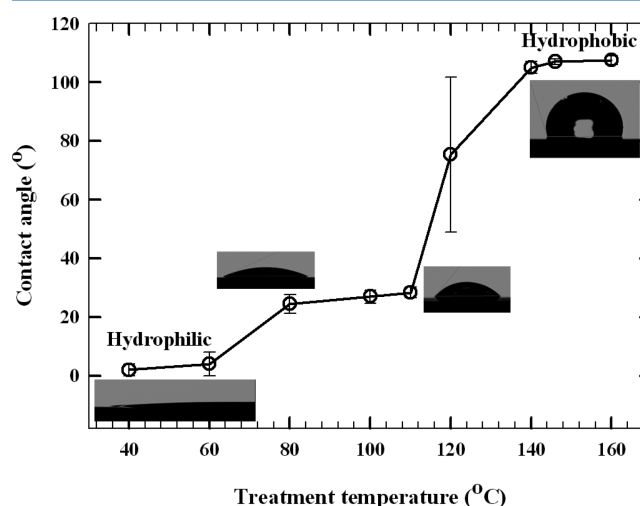


Figure 4. Surface wettability of heat-treated (annealed) ultrathin (10 nm) Nafion film. (Solid lines are only a guide for eye.) Error bar represents standard deviation of results obtained from four different points of each of triplicate samples.

It can be noted that the free surface wettability switches from super-hydrophilic for the unannealed film to hydrophobic for the 160 °C annealed film. The contact angle measurements of the unannealed films (dried at 40 °C) showed an almost spreading behavior. The same spreading behavior was observed even after further treatment at 60 °C. However, the films heat treated at 80, 100, and 110 °C showed a small but significant change in contact angle, which ranged 25–27°. Incidentally, 110 °C is slightly higher than the bulk Nafion T_g (109 °C).¹⁹ Upon heat treatment of the film at 120 °C, i.e., above the bulk Nafion T_g , a large variability in the surface wettability of the samples was observed. Some samples exhibited hydrophilic surface while others showed hydrophobic surface. Furthermore, in some cases, higher contact angle was observed initially, but it quickly changed into a smaller contact angle within a few seconds. It is noted that even the lowest contact angle observed for the 120 °C treated films were still higher than that of 110 °C treated films. Interestingly, upon increasing the treatment temperature by another 20 °C, i.e. annealing to 140 °C, the film surface changed to a stable hydrophobic surface with a contact angle of $105 \pm 2^\circ$. The water droplet exhibiting high contact angle did not spread for several minutes rather gradually evaporated with time. The highest water contact angle of 107° was observed for films heat treated at 146 °C. The contact

angle did not change with heat treatment at higher temperatures of up to 160 °C.

From the aforementioned results, several interesting insights may be gathered. First, a major surface rearrangement, which results in a stable state, occurred only upon heat treatment at temperatures far exceeding the bulk Nafion T_g . At the glass transition temperature, molecules attain sufficiently high mobility to transform from its glassy state to rubbery state, such that possible reorientation/reorganization may occur to minimize the surface energy and achieve thermodynamic stability. This is not entirely surprising, because for some thin polymer films due to favorable interaction with the substrate, the film T_g is observed to be higher than that of the bulk polymer.³² It must be noted that we did not examine the effect of thermal treatment time, which was kept constant in all our experiments. It is possible that the molecules may be mobile at 110 °C but not possess sufficiently high mobility to attain a relaxed state in the relatively short time. Nafion is made of two distinct components: a hydrophobic Teflon-like backbone and a side chain terminating with hydrophilic, sulfonate-group-containing moiety. The small but measurable change in wettability for samples heated at temperatures in 80–110 °C range compared to the unannealed film may be explained considering the mobility of the side chain, which is significantly more mobile than the bulk backbone. The extremely hydrophilic surface of the untreated films can be attributed to the large number of sulfonic groups extending outward. These mobile chains may fold down or hide away from the free surface upon thermal treatment at sufficiently high temperature. Since, the surface of films heat treated at temperatures in the 80–110 °C range is still hydrophilic, it is reasonable to deduce that a large number of hydrophilic side chains must still be present on the free surface. Finally, it is noticeable that the contact angle did not change further upon heat treatment at temperatures higher than 146 °C, which indicates that the maximum surface reorganization occurs at ~146 °C.

On the basis of the aforementioned discussions, a general conclusion can be drawn that the thermal treatment of the 10 nm Nafion film affects both the bulk (conductivity) and the free surface (wettability) properties simultaneously. Recalling that the 110 °C (correspond to bulk T_g) heat-treated film showed only a small change in surface wettability, the partial reduction in the bulk transport properties at the same film treatment condition is highly consistent with the simultaneous changes. On the other hand, the films that were thermally treated at 146 and 160 °C exhibit similar bulk and surface properties indicating complete surface and bulk reorganization to have occurred upon annealing at 146 °C. It is worth noting that our study is the first one to report that an elevated temperature treatment of Nafion ultrathin films has a significant impact on both surface wettability and its bulk proton conductivity.

The highly reduced conductivity of annealed thin films is confounding considering that almost membrane-like conductivity values have been reported for ionomers in CLs.^{30,31} As discussed earlier, fabrication of membrane electrode assembly (MEA) often requires a hot pressing step wherein the catalyst coated membrane (CCM) is pressed against porous carbon backing at 120–195 °C to minimize contact resistance and enhance durability. Also, MEA prepared by decal transfer technique involves high temperature (usually 130–210 °C) transferring process.^{33,34} Thus, if the ionomer in the CL was to exhibit property changes similar to that observed for our thin films, then for MEAs subjected to a hot-pressing step we should

expect a significantly poor electrochemical performance that is limited by proton-transport in the CL. Experimental evidence suggests that instead of a loss in performance, a performance enhancement is observed for MEAs subjected to hot pressing indicating that heat treatment or annealing does not have an adverse effect on CL ionomer conductivity.

To resolve this conundrum, we considered the local environment in the catalyst layer during actual operation. A fuel cell is typically “conditioned” during the startup and goes through a break-in period during which the electrochemical interfaces are activated. The activated cell during the operation generates water in the cathode catalyst layer, and as such, the liquid water can exist in the CL. The presence of liquid water is less clear on the anode side. The role of bulk liquid water present in the CL in proton conduction is an interesting question in itself and beyond the scope of this work. On the other hand, it is well-known that the Nafion membrane uptakes different amounts of water upon exposure to saturated water vapor and saturated liquid water.³⁵ More recently, Bass et al.⁷ have shown that the free surface of 100 nm film shows different GISAXS responses for surfaces when exposed to water vapor and to liquid water. Considering bundle-like micro/nanostructure, they hypothesized that the cylindrical bundles forming the skin of the film changed their orientation from parallel to perpendicular with respect to the surface. Such a movement of bundle is unlikely for a 10 nm thin film, wherein a 50–100 nm long bundle is unlikely to stand up, leaving free surface. Nonetheless, these observations point to the possibility of reorganization of structures and, therefore, properties upon exposure to liquid water.

Switchability of Surface Wettability upon Liquid Water Exposure. A set of experiments was performed to study the response of the annealed films that were exposed to liquid water as termed as regenerated film. It is important to clarify here that the film was not immersed in water to avoid any dissolution or floating away of the Nafion film as described in the Experimental Section. The contact angle and conductivity measurements were performed on the regenerated and second-time annealed film.

The contact angle results for four different films (categorized on the basis of treatment) are shown in Figure 5. The switching of free surface wettability upon annealing and exposure of liquid water is evident. Our experimental observation, free surface

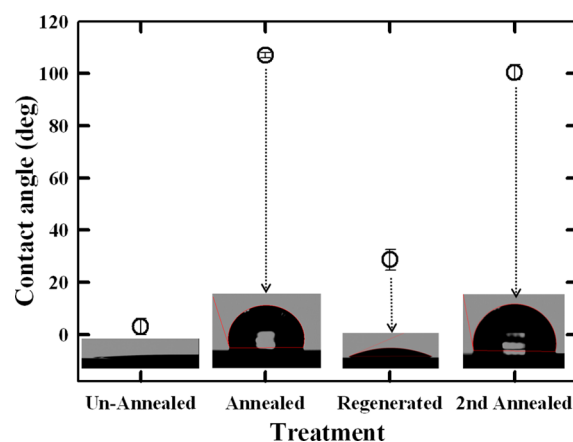


Figure 5. Switchability of surface wettability of ultrathin film subjected to thermal annealing (annealed film) and liquid water exposure (regenerated film).

switchability with local atmosphere, is consistent with the theoretical molecular dynamic simulation by Eikerling group.³⁶ We offer one possible explanation for the observations. Considering that the sulfonic group is the key contributor to hydrophilic free surface, it can be deduced that upon annealing the sulfonic group containing side-chains folds down (from the free surface) exposing a predominantly hydrophobic backbone to the air. Upon exposure to liquid water these sulfonic groups, known for their affinity for water, fold back up. Subsequent drying of this regenerated surface at low temperature does not result in the folding down of the side-chains, perhaps due to insufficient energy. Also, it is evident that prolonged exposure to saturated water vapor is not sufficient to induce the mobility of the sulfonic groups to the surface. Further, to support the bulk rearrangement along with surface, we investigated thickness effect on the wettability of water treated films considering film thickness, 10, 30, and 55 nm. Initially, three films converted from hydrophilic to hydrophobic due to elevated temperature annealing (at 146 °C). Interestingly, the regeneration process was found to be time-dependent indicating bulk rearrangement of the polymer. Upon 24 h water exposure, the 10 nm film switched back to hydrophilic, but the other two thicker films did not. In contrast, 48 h was needed for 30 nm film, and even higher exposure time of 96 h was needed for 55 nm film to regenerate. The slow regeneration for thicker film indicates that the process is highly related to the bulk reconfiguration or reorganization process. However, the time scales for these changes and the associated energetic would be an interesting topic for future study and are outside the scope of the current work.

Protonic Conductivity of Annealed and Regenerated Films. As discussed above, the surface wettability of the thin film undergoes changes upon thermal annealing but revert backs upon subsequent exposure to liquid water. To investigate how the film treatment conditions affect the ionomer film proton conduction, impedance measurements were carried out. The proton conductivity of the unannealed, first-time annealed, regenerated, and second-time annealed films at different RH and 60 °C is reported in Figure 6. Two interesting observations can be made. The regenerated film shows a remarkable recovery in protonic conductivity with values even greater than that of the unannealed film. As discussed above, the subsequent annealing of this regenerated film showed a switchable wettability back to hydrophobic free surface. Interestingly, the

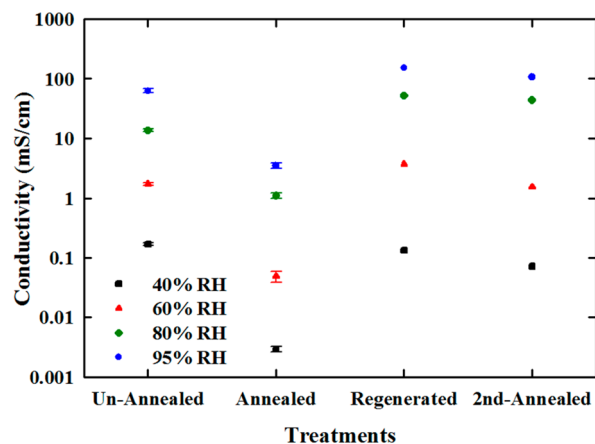


Figure 6. Proton conductivity for 10 nm Nafion film subjected to the various treatments.

protonic conductivity of this second-time annealed film does not get depressed as that observed for the first-time annealed film. In other words, even with a hydrophobic free surface, the protonic conductivity is not affected. This aspect is discussed further in the last subsection.

Activation Energy for Ionic Conduction. Measurement of proton conductivity at constant RH but different temperatures allowed the determination of activation energy for proton conduction. The activation energy can provide some insight on the similarities or differences in the mechanism for proton conduction among the unannealed, the annealed, and the regenerated films. The plots showing activation energy for the three differently treated films are presented in Figure 7. The

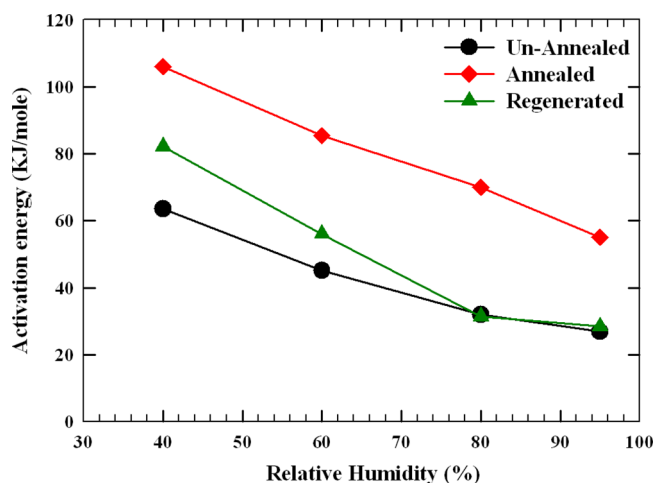


Figure 7. Activation energy as a function of RH for unannealed (black ●), annealed (red ◆), and regenerated (green ▲) films.

activation energy of annealed film was nearly two times compared to that of the unannealed films. This higher activation energy may be a result of less proton mobility due to less water uptake or some other intrinsic properties changes. At 95% RH, the activation energy of regenerated film is almost the same as that observed for unannealed film, but proton conductivity is higher in the regenerated film than that of unannealed film. On the other hand, proton conductivity for regenerated and unannealed films at 40% RH is comparable whereas significant differences in the activation energy can be noted.

Discussions on the Wettability Switching and Conductivity Regeneration. Some hypotheses and deductions can be made from these observations. Expectedly, annealing induces relaxation/reorganization of the polymer molecules. The relaxation comprises mobility of both the longer-chain backbone as well as the much shorter side-chains (~1 nm). Given the size and structure of the backbone and the side chain, it can be argued that the side chain mobility is faster than that of the backbone. The first-time annealing results in a major reorganization of the molecules (side chain) on the surface and in the bulk. Kongkanand¹⁰ found that the rate of water uptake for the annealed Nafion films was greatly reduced compared to that for the unannealed films. They attributed this to the formation of a hydrophobic skin at the free surface of the annealed film. Thus, it would be tempting to attribute the lower conductivity of annealed films to lower water uptake because of its hydrophobic skin. However, since the second-time annealed film, which also exhibits a hydrophobic surface, shows high

conductivity rules out that the hydrophobic skin is primarily responsible for low conductivity. A possible explanation of low proton conductivity of first time annealed may be the formation of static crystalline domain due to high temperature annealing as discussed by Modestino et al.¹² on the basis of GISAXS measurement of thin ionomer film. They suggested that the static domain may impede water uptake and could be a reason for significant reduction of proton conductivity. Without microstructural information, any further hypothesis regarding annealing and regeneration due to liquid water contact will be highly speculative. On the other hand, this is the first study to bridge the seeming disconnect between highly depressed protonic conductivity of annealed films and the observed, much-higher catalyst layer ionic conductivity. Since the ionomer in the CL will experience liquid water during actual cell operation, even if the annealed ionomer film had low initial conductivity, upon its exposure to liquid water the conductivity is expected to increase dramatically. It is acknowledged that our study was carried out on ionomer film self-assembled on planar substrate of thermally grown SiO₂, which differs in surface chemistry and geometry of the Pt/C particles. It is instructive to point out that similar study on planar carbon or Pt substrate would preclude the measurements of ionic conductivity because of the electronically conductive Pt or C substrate. Further, the ionomer film in an actual catalyst layer may not be uniformly distributed and may be both discontinuous and of varying thickness. With these uncertainties, it is difficult to extract meaningful conductivity values or make conclusions about film properties, which we have shown are thickness-dependent.^{13,14}

CONCLUSIONS

It can be concluded that thermal annealing of the 10 nm ultrathin Nafion film results in a reorientation or reorganization altering the surface and bulk properties. With increasing treatment temperature, surface wettability switches from super-hydrophilic to hydrophobic while bulk proton conductivity reduces significantly. No differences in the wettability and proton conductivity were observed for films annealed at 146 and 160 °C, indicating that all restructuring/reorganization was attained upon annealing at 146 °C. The most interesting finding of this study is that, upon liquid water exposure, the hydrophobic skin of the annealed film switches back to the hydrophilic surface. Further, the liquid-water exposed annealed film exhibits an even higher proton conductivity compared to the unannealed or as-prepared film. Subsequent heat treatment of the liquid water exposed film again turns the film skin hydrophobic, but the proton conductivity is not suppressed as in the case of the first heat treatment. This phenomenon has a direct implication for understanding the ionomer surface wettability and bulk conduction in the CL, which is subjected to thermal annealing during hot pressing and liquid water exposure during cell operation.

AUTHOR INFORMATION

Corresponding Author

*E-mail: kkaran@ucalgary.ca. Phone: 1-403-220-5754. Fax: 1-403-284-4852.

Notes

The authors declare no competing financial interest.

ACKNOWLEDGMENTS

The financial assistance for this work was provided by the Natural Sciences and Engineering Research Council of Canada (NSERC) for KK's Discovery Grant and Automotive Partnership Canada via Catalysis Research for Polymer Electrolyte Fuel Cells (CarPE-FC) Network.

REFERENCES

- (1) Holdcroft, S. Fuel Cell Catalyst Layers: A Polymer Science Perspective. *Chem. Mater.* Article ASAP.
- (2) More, K.; Borup, R.; Reeves, K. Identifying Contributing Degradation Phenomena in PEM Fuel Cell Membrane Electride Assemblies Via Electron Microscopy. *ECS Trans.* **2006**, *3*, 717–733.
- (3) Dura, A. J.; Murthi, S. V.; Hartman, M.; Satija, K. S.; Majkrzak, F. C. Multilamellar Interface Structures in Nafion. *Macromolecules* **2009**, *42*, 4769–4774.
- (4) Wood, L. D.; Chlistunoff, J.; Majewski, J.; Borup, L. R. Nafion Structural Phenomena at Platinum and Carbon Interfaces. *J. Am. Chem. Soc.* **2009**, *131*, 18096–18104.
- (5) Siroma, Z.; Kakitsubo, R.; Fujiwara, N.; Ioroi, T.; Yamazaki, S.-I.; Yasuda, K. Proton conductivity along interface in thin cast film of Nafion. *J. Power Sources* **2009**, *189*, 994–998.
- (6) Bass, M.; Berman, A.; Singh, A.; Konovalov, O.; Freger, V. Structure of Nafion in Vapor and Liquid. *J. Phys. Chem. B* **2010**, *114*, 3784–3790.
- (7) Bass, M.; Berman, A.; Singh, A.; Konovalov, O.; Freger, V. Surface-Induced Micelle Orientation in Nafion Films. *Macromolecules* **2011**, *44*, 2893–2899.
- (8) Paul, D. K.; Fraser, A.; Karan, K. Towards the understanding of proton conduction mechanism in PEMFC catalyst layer: Conductivity of adsorbed Nafion films. *Electrochem. Commun.* **2011**, *13* (8), 774–777.
- (9) Paul, D. K.; Fraser, A.; Pearce, J.; Karan, K. Understanding the Ionomer Structure and the Proton Conduction Mechanism in PEFC Catalyst Layer: Adsorbed Nafion on Model Substrate. *ECS Trans.* **2011**, *41*, 1393–1406.
- (10) Kongkanand, A. Interfacial Water Transport Measurements in Nafion Thin Films Using a Quartz-Crystal Microbalance. *J. Phys. Chem. C* **2011**, *115*, 11318–11325.
- (11) Dishari, K. S.; Hickner, M. A. Antiplasticization and Water Uptake of Nafion Thin Films. *ACS Macro Lett.* **2012**, *1*, 291–295.
- (12) Modestino, M. A.; Kusoglu, A.; Hexemer, A.; Weber, A. Z.; Segalman, R. A. Controlling Nafion Structure and Properties via Wetting Interactions. *Macromolecules* **2012**, *45*, 4681–4688.
- (13) Modestino, M. A.; Paul, D. K.; Dishari, S.; Petrina, S. A.; Allen, F. I.; Hickner, M. A.; Karan, K.; Segalman, R. A.; Weber, A. Z. Self-Assembly and Transport Limitations in Confined Nafion Films. *Macromolecules* **2013**, *46* (3), 867–873.
- (14) Paul, D. K.; Karan, K.; Giorgi, J.; Docoslis, A.; Pearce, J. Characteristics of Self-Assembled Ultrathin Nafion Films. *Macromolecules* **2013**, *46* (9), 3461–3475.
- (15) Schmidt-Roh, K.; Chen, Q. Parallel cylindrical water nano-channels in Nafion fuel-cell membranes. *Nat. Mater.* **2008**, *7*, 75–83.
- (16) Abuin, G. C.; Fuertes, M. C.; Corti, H. R. Substrate effect on the swelling and water sorption of Nafion nanomembranes. *J. Membr. Sci.* **2013**, *428*, S07–S15.
- (17) Ma, C.-H.; Yu, T. L.; Lin, H.-L.; Huang, Y.-T.; Chen, Y.-L.; Jeng, U.-S. Morphology and properties of Nafion membranes prepared by solution casting. *Polymer* **2009**, *50*, 1764–1777.
- (18) Ngo, T. T.; Yu, T. L.; Lin, H.-L. Influence of the composition of isopropyl alcohol/water mixture solvents in catalyst ink solutions on proton exchange membrane fuel cell performance. *J. Power Sources* **2013**, *225* (1), 293–303.
- (19) Yeo, S. R.; McBreen, J.; Kissel, G.; Kulesa, F.; Srinivasan, S. Perfluorosulphonic acid (Nafion) membrane as a separator for an advanced alkaline water electrolyser. *J. Appl. Electrochem.* **1980**, *10*, 741–747.

- (20) Liang, Z. X.; Zhao, T. S.; Xu, C.; Xu, J. B. Microscopic characterizations of membrane electrode assemblies prepared under different hot-pressing conditions. *Electrochim. Acta* **2007**, *53*, 894–902.
- (21) Zhang, J.; Yin, G.-P.; Wang, Z.-B.; Lai, Q.-Z.; Cai, K.-D. Effects of hot pressing conditions on the performances of MEAs for direct methanol fuel cells. *J. Power Sources* **2007**, *165*, 73–81.
- (22) Lin, J.-C.; Lai, C.-M.; Ting, F.-P.; Chyou, S.-D.; Hsueh, K.-L. Influence of hot-pressing temperature on the performance of PEMFC and catalytic activity. *J. Appl. Electrochem.* **2009**, *39*, 1067–1073.
- (23) Tsui, O. K. C.; Russell, T. P.; Hawker, C. J. Effect of Interfacial Interactions on the Glass Transition of Polymer Thin Films. *Macromolecules* **2001**, *34*, 5535–5539.
- (24) Jiang, X. Q.; Yang, C. Z.; Tanaka, K.; Takahara, A.; Kajiyama, T. Effect of chain end group on surface glass transition temperature of thin polymer film. *Phys. Lett. A* **2001**, *281*, 363–367.
- (25) Feng, Y.; Karim, A.; Weiss, R. A.; Douglas, J. F.; Han, C. C. Control of Polystyrene Film Dewetting through Sulfonation and Metal Complexation. *Macromolecules* **1998**, *31*, 484.
- (26) Sauer, B. B.; McLean, R. S. AFM and X-ray Studies of Crystal and Ionic Domain Morphology in Poly(ethylene-co-methacrylic acid) Ionomers. *Macromolecules* **2000**, *33*, 7939.
- (27) Hill, A. T.; Carroll, L. D.; Czerw, R.; Martin, W. C.; Perahia, D. Atomic Force Microscopy Studies on the Dewetting of Perfluorinated Ionomer Thin Films. *J. Polym. Sci., Part B: Polym. Phys.* **2003**, *41*, 149–158.
- (28) Srolovitz, D. J.; Safran, S. A. Capillary instabilities in thin films. I. Energetics. *J. Appl. Phys.* **1986**, *60*, 247.
- (29) Brochard, F.; Dalliant, J. Drying of solids wetted by thin liquid films. *Can. J. Phys.* **1990**, *68*, 1084.
- (30) Liu, Y.; Murphy, M. W.; Baker, D. R.; Gu, W.; Ji, C.; Jorne, J.; Gasteiger, H. A. Proton Conduction and Oxygen Reduction Kinetics in PEM Fuel Cell Cathodes: Effects of Ionomer-to-Carbon Ratio and Relative Humidity. *J. Electrochem. Soc.* **2009**, *156*, B970.
- (31) Boyer, C.; Gamburzev, S.; Velev, O.; Srinivasan, S.; Appleby, A. Measurements of proton conductivity in the active layer of PEM fuel cell gas diffusion electrodes. *Electrochim. Acta* **1998**, *43*, 3703.
- (32) Zhu, L.; Wang, X.; Gu, Q.; Chen, W.; Sun, P.; Xue, G. Confinement-Induced Deviation of Chain Mobility and Glass Transition Temperature for Polystyrene/Au Nanoparticles. *Macromolecules* **2013**, *46*, 2292–2297.
- (33) Wilson, M. S.; Valerio, J. A.; Gottesfeld, S. Low platinum loading electrodes for polymer electrolyte fuel cells fabricated using thermoplastic ionomers. *Electrochim. Acta* **1995**, *40*, 355.
- (34) Song, S. Q.; Liang, Z. X.; Zhou, W. J.; Sun, G. Q.; Xin, Q.; Stergiopoulos, V.; Tsiakaras, P. Direct methanol fuel cells: The effect of electrode fabrication procedure on MEAs structural properties and cell performance. *J. Power Sources* **2005**, *145*, 495.
- (35) Zawodzinski, T. A.; Gottesfeld, S.; Shoichet, S.; McCarthy, T. J. The Contact-Angle between Water and the Surface of Perfluorosulfonic Acid Membranes. *J. Appl. Electrochem.* **1993**, *23*, 86–88.
- (36) Malek, K.; Mashio, T.; Eikerling, M. Microstructure of Catalyst Layers in PEM Fuel Cells Redefined: A Computational Approach. *Electrocatalysis* **2011**, *2* (2), 141–157.